# Synthesis, characterisation and antibacterial effects of sol–gel derived biphasic calcium phosphate nanopowders

*Zahra Nazemi[1], Masoumeh Haghbin Nazarpak[2,3], Mehdi Mehdikhani-Nahrkhalaji[4], Hamid Staji[5], Mohammad Mehdi Kalani[1]*

[1]*Department of Material and Metallurgical Engineering, Semnan University, Semnan 35131-19111, Iran*
[2]*New Technologies Research Center (NTRC), Amirkabir University of Technology, Tehran 15875-4413, Iran*
[3]*Mawson Institute, University of South Australia, Mawson Lakes, Adelaide, South Australia 5095, Australia*
[4]*Department of Biomedical Engineering, Faculty of Engineering, University of Isfahan, Isfahan 81746-73441, Iran*
[5]*Department of Veterinary Medicine, Semnan University, Semnan 35131-19111, Iran*
*E-mail: haghbin@aut.ac.ir*

Published in Micro & Nano Letters; Received on 6th November 2013; Revised on 26th April 2014; Accepted on 13th May 2014

Hydroxyapatite (HA) and β-tricalcium phosphate (β-TCP) represent the main types of calcium phosphates used for the reconstruction of bone defects in maxillofacial, dental, orthopaedic and drug delivery applications. The bioactivity and bioresorbability of biphasic calcium phosphate (BCP) ceramics can be controlled by varying the HA/β-TCP ratio. In this reported work, BCP nanopowders were prepared by a simple sol–gel method, in which $Ca(NO_3)_2 \cdot 4H_2O$ and $P_2O_5$ were used as precursors for calcium and phosphate, respectively. The different phase ratios of HA/β-TCP were obtained by changing the sintering temperature. X-ray diffraction, inductive coupled plasma-atomic emission spectroscopy, scanning electron microscopy, transmission electron microscopy and Fourier transformer infrared spectrophotometer results have shown that increasing the sintering temperature could cause more decomposition of HA into β-TCP. Moreover, the size of the prepared nanoparticles was measured between 10 and 500 nm. Finally, the antibacterial activity was studied using *Escherichia coli* (ATCC 25922) as the Gram-negative bacteria. The antibacterial effect of the BCP sample with 50% HA–50%β-TCP phase ratio was tested at concentrations of 100, 200 and 300 mg/ml. The results showed bacterial growth reduction at a concentration of 300 mg/ml, which makes it a good candidate for the treatment of bone defects.

**1. Introduction:** Many biomaterials have been suggested to repair osseous defects and restore bone damage [1]. Hydroxyapatite [HAp, $Ca_{10}(PO_4)_6(OH)_2$] and β-tricalcium-phosphate [β-TCP, $\beta\text{-}Ca_3(PO_4)_2$] are widely recognised as potential bioceramics for both dental and orthopaedic applications because of their close chemical similarity with the inorganic component of vertebrate bone and tooth mineral [2, 3]. Despite their favourable biological properties, both materials have a number of drawbacks that reduce their clinical performance. In vivo and in vitro dissolution experiments have indicated that the dissolution of HAp in the human body after implantation is too low to achieve the optimal formation of bone tissue. On the other hand, β-TCP shows fast release of $Ca^{2+}$ and $PO_4^{3-}$ ions when exposed to physiological fluids. This fast dissolution profile drastically reduces the surface area available for bone cell proliferation, and therefore its application in the clinical setting is limited [4]. Therefore biphasic calcium phosphate (BCP) consisting of HA and TCP can be used to control the bioresorbability and achieve optimal results [1, 5, 6]. It has been shown that the bone in growth into BCP ceramic particles is rapid. The bone in the growth process has been revealed by the two-stage physicochemical events occurring after implantation of BCP, that is, crystal dissolution and the precipitation of biological apatite [1].

The bioactivity of calcium phosphate materials depends on many factors during the synthesis procedure including precursor reagents, impurity contents, crystal size and morphology, concentration and the mixture order of reagents, pH and temperature. Such conditions are application specific and should be controlled by synthesis preparation parameters [6]. There are many techniques for the production of BCP including wet chemical methods [3, 7], microwave irradiation [1, 6], combustion processing [8], the co-precipitation technique [4], preparation from natural resource [9], sol–gel synthesis [5], hydrothermal processes, solid-state reaction, spray pyrolysis and treatment of natural bone. Among them, the sol–gel method is regarded as the promising way for convenient synthesis because it requires less equipment used, has high output and easy operation processes [5]. Moreover, the sol–gel product is characterised by nanosize dimensions of the primary particles. This small domain is a very important parameter for improvement of the contact reaction and the stability at the artificial/natural bone interface. Moreover, the high reactivity of the sol–gel powder allows a reduction of processing temperature and any degradation phenomena occurring during sintering [10].

For the past few years, prophylactic measures to prevent postoperative infections have probably been contributing to limit orthopaedic implant infections (OII) in orthopaedic surgery. *Staphylococci* are the main microorganisms implicated in OII and prophylaxis is generally directed against these pathogens. *Escherichia coli* (*E. coli*) is the second most common cause of Gram-negative OII (20–30%) [11].

Although the antibacterial activity of HA has been evaluated, previously [12], this was the first time that BCP antibacterial activity has been evaluated.

The aim of this study was first to evaluate the effect of sintering temperature on the phase ratio (HA/β-TCP) of BCP prepared by a simple sol–gel method. Then, the best composition based on the proper phase ratio (HA/β-TCP) was selected for an antibacterial test on *E. coli* as the second most common cause of Gram-negative OII. Moreover, the minimum bactericidal concentration (MBC) value for BCP nanopowders was determined.

Such composition providing a proper antibacterial effect can be a good candidate for dental and orthopaedic applications.

## 2. Materials and methods

2.1. Preparation of BCP nanopowders: The sol–gel route was used to synthesise BCP samples. Calcium nitrate tetrahydrate

**Table 1** Samples' code, their phase ratio and heat treatment characterisation

| Sample code | Sintering temperature, °C | HA, % | β-TCP, % | CaO, % |
|---|---|---|---|---|
| BCP1 | 820 | 76.6 | 15 | 8.4 |
| BCP2 | 950 | 80 | 20 | 0 |
| BCP3 | 1050 | 50 | 50 | 0 |
| BCP4 | 1150 | 94 | 6 | 0 |

($Ca(NO_3)_2 \cdot 4H_2O$, Merck) and phosphoric pentoxide ($P_2O_5$, Merck) were used as green material precursors for calcium and phosphorus. Briefly, to produce 2 g of pure HA powder, 4.7 g of $Ca(NO_3)_2 \cdot 4H_2O$ and 0.84 g of $P_2O_5$ were dissolved in anhydrous ethanol (Merck) separately. The solutions were mixed in a Ca/P molar ratio of 1.67 as an initial mixed precursor solution. The solution mixtures were continuously stirred for 24 h at ambient temperature. Then the white transparent derived gel was dried at 85°C for 24 h in an electrical air oven [10]. Sintering of dried gel samples was performed at 820, 950, 1050 and 1150°C for 7 h. The heating rate did not exceed 5°C/min.

The samples' code, phase ratio and heat treatment characterisation of the prepared powders are given in Table 1.

2.2. Characterisation: The phase composition and crystallinity of the prepared BCP nanoparticles were analysed by X-ray diffraction (XRD) using a D8-ADVANCE Bruker apparatus CuKα wavelength of 0.15406 nm, with a $2\theta$ range of 20°–80°. Moreover, the infrared spectra of the prepared BCP nanoparticles were obtained using a Fourier transformer infrared spectrophotometer (FTIR, SHIMADZU). The morphology of the synthesised BCP was studied and evaluated by scanning electron microscopy (SEM) (KYKY-EM3200). Transmission electron microscopy (TEM) (Zeiss – EM10C – 80 KV) was utilised to study and determine the size and morphology of the nanoparticles. The elemental analysis was performed by inductively coupled plasma-atomic emission spectroscopy (Intagra XL, GBC).

2.3. Antibacterial activity: Tryptic soy broth (TSB, Merck) was used as the culture medium. BCP3 nanopowders were first mixed with the broth. The final sample concentrations tested were 100, 200 and 300 mg/ml of broth. Then, these suspensions were autoclaved at 121°C temperature and 15 psi for 15 min to be sterilised. The bacterial broth dilution method documented in the National Committee for Clinical Laboratory Standards publication, M7-T2, was used as a bacterial susceptibility test to determine the MBC of BCP3 nanopowders. These mixtures were then added to standard inoculums of the microorganisms ($1.5 \times 10^7$ bacteria/ml) that were prepared according to McFarland standard No. 0.5 in 0.01 dilution. Bacterial cultures without BCP3 nanopowders served as controls. The viability levels of the bacterial suspensions incubated with different concentrations of BCP3 nanopowders were assessed using pour plates in nutrient agar. Assessments was performed after 24, 48, 72, 96 and 120 h of cultivation in broth containing nanopowders, also 0.1 ml of the suspensions were poured onto nutrient agar plates. The antibacterial activity of each tube was assessed three times. The growth of bacteria was evaluated after cultivation on nutrient agar at 37°C for 24 h. Absence of growth on the plates (0) was an indicator of the bactericidal effect of given BCP3 nanopowders. Very sparse, sparse and moderate growths (1, 2 and 3, respectively) indicated that the material had a growth inhibitory effect. Good growth (4) on a plate was taken to indicate no effects [13, 14]. At each interval, pH changes of the broth containing the BCP nanopowders were measured.

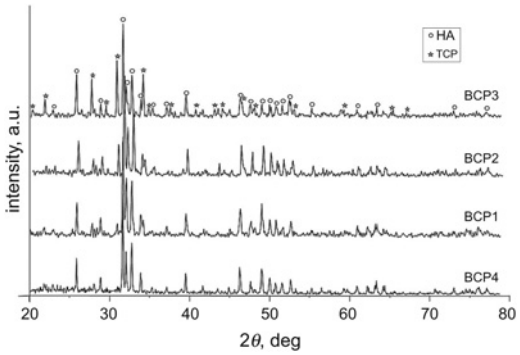


**Figure 1** *XRD patterns of BCPs with different HA/β-TCP ratios*

**3. Results and discussion:** XRD patterns of the sol–gel prepared powders are shown in Fig. 1. The results showed that sintering temperature plays an important role in the formation of the β-TCP phase. The *d* spacing was compared with the standard data (JCPDS). XRD patterns of the sol–gel prepared BCP samples were matched with the hexagonal HA (JCPDS No. 9-432) and β-TCP (JCPDS No. 9-169) crystals. There are three phases in BCP1 samples sintered at 820°C. An additional CaO phase was removed by sintering at temperatures higher than 820°C and there only remained HA and β-TCP phases. The phase ratios of HA/β-TCP in the BCP1 and BCP2 samples are nearly close to each other. As the sintering temperature is increased up to 1050°C, several peaks of the XRD pattern which belong to the β-TCP powder become more distinct. So the maximum amount of the β-TCP phase has been achieved at 1050°C temperature. A desirable phase ratio having equal amounts of two phases appeared in the BCP3 sample (50% HA–50%β-TCP). On the other hand, the temperature transition from 950 to 1050°C can be considered as a critical temperature range for HA decomposition and β-TCP phase formation. It was clear that by increasing sintering temperature up to 1150°C, the amount of the HA phase was enhanced further, which is in agreement with previous studies [15].

On the other hand, the result of XRD showed less width and sharp height peaks by increasing temperature from 820 to 1150°C. The broad and weak diffraction peaks indicate a poor crystallinity [16]. In fact, the higher sintering temperature could result in more crystalline samples.

The mean crystallite size (*D*) of the particles was also calculated from the XRD line broadening measurement from the Scherrer equation (1) [17].

The grain size was in nanometre scale. Moreover, the results showed that by increasing the temperature process from 950 to 1150°C, the particle size of powder increased (Table 2).

Fig. 2 shows the FTIR absorption spectra of the prepared powders. In this Figure, the O–H stretching and vibrating band are found in the region at about 3580 and 635 $cm^{-1}$ in the samples, respectively, which confirm the presence of HA formation in the powder composition [18–20]. The stretching band of $HPO_4^{2-}$ at the 970 $cm^{-1}$ wavelength is attributed to the β-TCP structures [6]. The strongest bands at about 926–1105 $cm^{-1}$ in all samples were assigned to the P–O stretching vibration of the phosphate groups ($PO_4^{3-}$). $PO_4^{3-}$ bands at 553, 572 and 602 $cm^{-1}$ and about 1030–1090 $cm^{-1}$ are also

**Table 2** Mean crystalline size of sol–gel prepared particles that were determined by using Scherer's equation

| Sample code | Mean crystalline size, nm |
|---|---|
| BCP1 | 48 |
| BCP2 | 48 |
| BCP3 | 49 |
| BCP4 | 63 |




doi: 10.1049/mnl.2013.0655

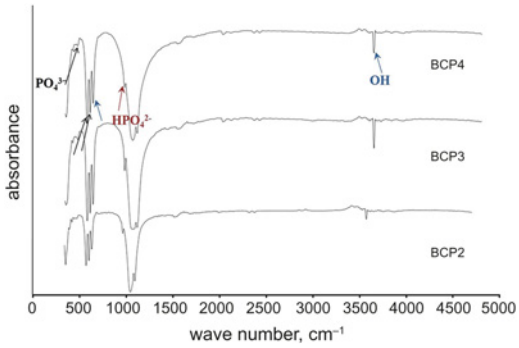


**Figure 2** *FTIR spectrometer curves of samples*

attributed to the presence of the HA phase in compositions [21]. The broadening bands at 3000–3700 $cm^{-1}$ are attributed to absorbed water in the compositions [12]. The FTIR results confirmed the formation of both the HA and the β-TCP phases beside each other in all samples, which confirm the XRD results.

The elemental analysis by ICP-AES for the three powders is presented in Table 3. According to the results, the weight ratios of Ca/P (wt%) were 2.04, 1.9 and 2.1 in the BCP2, BCP3 and BCP4 samples, respectively. Such results are acceptable regarding the XRD analysis.

SEM analysis of BCP2 and BCP3 are illustrated in Figs. 3*a* and *b*. As can be seen, both the powders exhibited tiny agglomerations of nanoparticles. The particle size of the BCP2 and BCP3 samples were about 15–70 and 10–500 nm, respectively. Moreover, it is obvious that powders sintered at lower temperature (BCP2) became finer and more homogeneous than for other samples. A prolate spheroidal shape morphology could be observed at some BCP3 powders.

Moreover, the TEM result confirms the SEM results that the synthesised BCP4 powders are nanosized (Fig. 4). There are very fine particles with <10 nm size in this Figure. Certain agglomeration of BCP particles was also observed. Such agglomeration can be attributed to the high surface area of nanoparticles and their high sintering temperature in the synthesis process.

**Table 3** Elemental concentration (wt%) of three different powders

| Sample code | Ca, wt% | *P*, wt% |
|---|---|---|
| BCP2 | 38.7 | 18.9 |
| BCP3 | 38 | 19.1 |
| BCP4 | 38.2 | 18.2 |

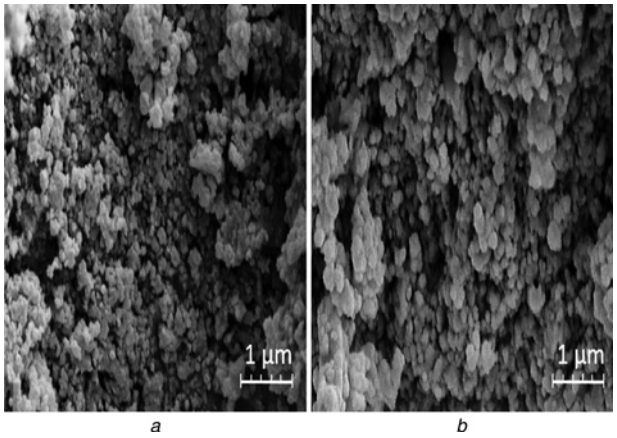


**Figure 3** *SEM image from BCP2 and BCP3 samples*
*a* BCP2
*b* BCP3

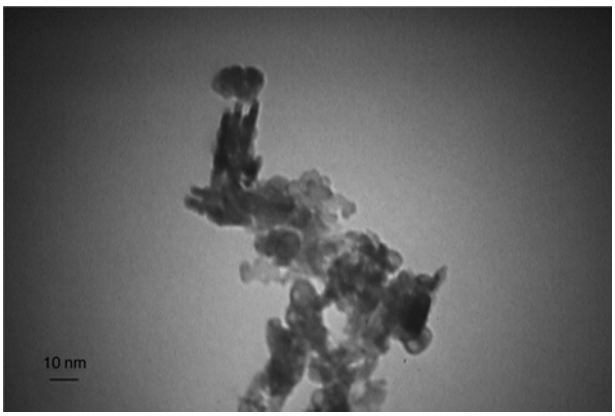


**Figure 4** *TEM image of BCP4 powders*

BCP3 nanopowders were chosen for antibacterial assay because of its suitable phase ratio. This sample has equal percentage of both stable HA and resorbable β-TCP phases.

The results from the antibacterial test revealed that the BCP3 sample at concentrations of 100 and 200 mg/ml showed no antibacterial activity and had similar behaviour as the control sample; however, no viable colonies could be observed after four days for BCP3 at a concentration of 300 mg/ml (Fig. 5). Hence, the MBC for this sample was achieved at 300 mg/ml concentration.

pH and charge gradients are important in prokaryotic physiology in terms of generating a proton motive force. Most organisms have a pH range in which preferential growth occurs and several sophisticated systems operate that can affect both the intra- and the extracellular environment [22]. Given the results of previous studies in an alkaline pH as generated by a biomaterial could be responsible for the antibacterial effect [13, 23, 24].

Fig. 6 shows pH variations in the broths containing BCP3 nanopowders. The initial pH of the broth was 7.3. The broth containing BCP3 showed a pH rise to 7.96, 8.08 and 8.32 for 100, 200 and 300 mg/ml concentrations, respectively, after 120 h. pH reached 7.8 at a 300 mg/ml concentration, after 96 h.

From the other point of view, pH regulation will effect the growth and development of a variety of cells, including osteoblasts and osteoclasts, processes of mineralisation and the repair of skeletal tissues [25, 26]. According to previous studies, the obtained pH in this study has no harmful effects and it is a reliable range. For example, Okabe *et al.* [27] observed that the alkaline pH (7.8) stimulates ALP activity and calcified nodule formation on human dental pulp cells. Furthermore, the mineralisation activity of these cells was enhanced by alkaline pH conditions. Arnett and Spowage [28] indicated that, under certain conditions, the pH difference in the osteoclast environment could result in appreciable alterations in bone resorption. Very slight alterations in ambient hydrogen ion concentration can effectively 'switch on' or 'switch

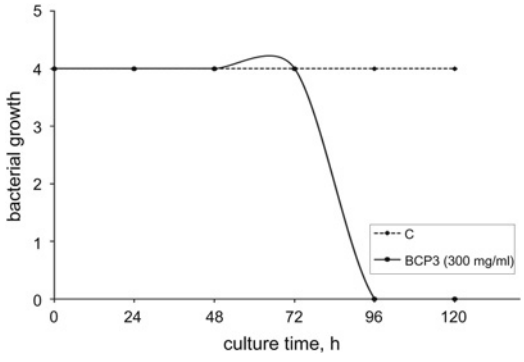


**Figure 5** *Effect of BCP3 nanopowders on growth of E. coli*

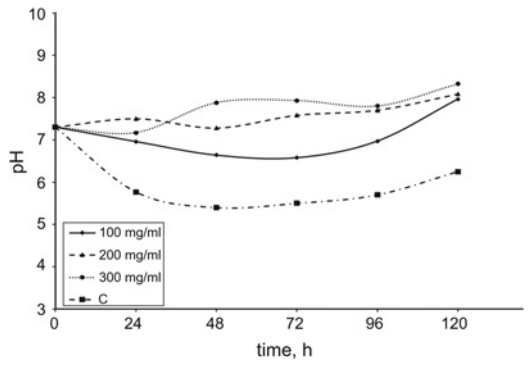


**Figure 6** *pH changes of broth containing BCP3 nanopowders*

off' rat osteoclasts in vitro, which conceivably may provide some perception of the pathogenesis of remodelling disorders such as osteoporosis. Mature rat and human osteoclasts were observed to be almost inactive at 'physiological' or blood pH (7.4), but resorption pit formation increased steeply as the pH reached to about 6.8. Moreover, acidification progressively reduced the mineralisation of bone nodules and osteoblast proliferation and collagen synthesis were unaffected by pH in the range of 7.4 to 6.9 [29].

In this work, pH levels did not rise to higher values; however, antibacterial activity was observed. It could be deduced that such materials will not have any harmful effect in the activity of cells; however, they deserve further investigation for their antibacterial activity

$$D = 0.89\lambda/\beta\cos\theta \quad (1)$$

where $\lambda$ is the wavelength (CuK$\alpha$) and $\beta$ is the width of the peak in the middle of its height and $\theta$ is the diffraction angle.

**4. Conclusion:** The sol–gel method provides a simple route for the synthesis of BCP nanopowders. The phase ratio of the composition is dependent on the sintering temperature at a constant time. The fraction of the β-TCP phase increased by increasing the sintering temperature up to 1050°C, but higher temperatures up to 1150°C had an adverse result. By this synthesis method, BCP nanoparticles in the range of 10–500 nm were obtained. Moreover, the antibacterial study demonstrated that the MBC of BCP3 nanopowders for *E. coli* were 300 mg/ml; pH changes were 7.3–8.32 at this concentration.

The prepared crystalline BCP nanopowders were able to improve the contact reaction and the stability at the artificial/natural bone interface for medical applications. These biomaterials have also been proposed for use in bone drug-delivery systems intended to release various therapeutic agents in situ.

These compositions will be investigated as local drug delivery systems in the near future.

**5. Acknowledgment:** The authors acknowledge M. Kanani for assistance in the bacterial culture studies.

## 6 References

[1] Manjubala I., Sivakumar M.: 'In-situ synthesis of biphasic calcium phosphate ceramics using microwave irradiation', *Mater. Chem. Phys.*, 2001, **71**, pp. 272–278

[2] Rameshbabu N., Prasad Rao K.: 'Microwave synthesis, characterization and in-vitro evaluation of nanostructured biphasic calcium phosphates', *Curr. Appl. Phys.*, 2009, **9**, pp. 529–531

[3] Kannan S., Ventura J.M.G., Lemos A.F., Barba A., Ferreira J.M.F.: 'Effect of sodium addition on the preparation of hydroxyapatites and biphasic ceramics', *Ceram. Int.*, 2008, **34**, pp. 7–13

[4] Kim T.W., Park Y.M., Kim D.H., *ET AL.*: 'In situ formation of biphasic calcium phosphates and their biological performance in vivo', *Ceram. Int.*, 2012, **38**, pp. 1965–1974

[5] Chen J., Wang Y., Chen X., *ET AL.*: 'A simple sol–gel technique for synthesis of nanostructured hydroxyapatite, tricalcium phosphate and biphasic powders', *Mater. Lett.*, 2011, **65**, pp. 1923–1926

[6] Farzadi A., Solati-Hashjin M., Bakhshi F., Aminian A.: 'Synthesis and characterization of hydroxyapatite/β-tricalcium phosphate nanocomposites using microwave irradiation', *Ceram. Int.*, 2011, **37**, pp. 65–71

[7] Kannan S., Ventura J.M.G., Ferreira J.M.F.: 'Synthesis and thermal stability of potassium substituted hydroxyapatites and hydroxyapatite/β-tricalciumphosphate mixtures', *Ceram. Int.*, 2007, **33**, pp. 1489–1494

[8] Aghayan M.A., Rodríguez M.A.: 'Influence of fuels and combustion aids on solution combustion synthesis of bi-phasic calcium phosphates (BCP)', *Mater. Sci. Eng. C*, 2012, **32**, pp. 2464–2468

[9] Balázsi C., Wéber F., Kövér Z., Horváth E., Németh C.: 'Preparation of calcium-phosphate bioceramics from natural resources', *J. Eur. Ceram. Soc.*, 2007, **27**, pp. 1601–1606

[10] Fathi M.H., Hanifi A.: 'Evaluation and characterization of nanostructure hydroxyapatite powder prepared by simple sol–gel method', *Mater. Lett.*, 2007, **61**, pp. 3978–3983

[11] Cremet L., Corvec S., Bemer P., *ET AL.*: 'Orthopaedic-implant infections by *Escherichia coli*: molecular and phenotypic analysis of the causative strains', *J. Infect.*, 2012, **64**, pp. 169–175

[12] Thian E.S., Lim P.N., Konishi T., *ET AL.*: 'Zinc-substituted hydroxyapatite: a biomaterial with enhanced bioactivity and antibacterial properties', *J. Mater. Sci., Mater. Med.*, 2013, **24**, pp. 437–445

[13] Mortazavi V., Mehdikhani Nahrkhalaji M., Fathi M.H., Mousavi S.B., Esfahani B.N.: 'Antibacterial effects of sol–gel-derived bioactive glass nanoparticle on aerobic bacteria', *J. Biomed. Mater. Res. A*, 2010, **94**, pp. 160–168

[14] Munukka E., Lepparanta O., Korkeamaki M., Vaahtio M., Peltola T., Zhang D.: 'Bactericidal effects of bioactive glasses on clinically important aerobic bacteria', *J. Mater. Sci. Mater. Med.*, 2008, **19**, pp. 27–32

[15] Gomes S., Nedelec J.M., Renaudin G.: 'On the effect of temperature on the insertion of zinc into hydroxyapatite', *Acta Biomater.*, 2012, **8**, pp. 1180–1189

[16] Moghimian P., Najafi A., Afshar S., Javadpour J.: 'Effect of low temperature on formation mechanism of calcium phosphate nano powder via precipitation method', *Adv. Powder Technol.*, 2012, **23**, pp. 744–757

[17] Azaroff L.A.: 'Elements of X-ray crystallography' (McGraw-Hill, New York, 1968), pp. 38–42

[18] Khelendra A., Singh G., Puri D., Prakash S.: 'Synthesis and characterization of hydroxyapatite powder by sol–gel method for biomedical application', *J. Miner. Mater. Charact. Eng.* , 2011, **10**, pp. 727–734

[19] Weng W., Baptista J.L.: 'Sol–gel derived porous hydroxyapatite coatings', *J. Mater. Sci., Mater. Med.*, 1998, **9**, pp. 159–163

[20] Kannana S., Vieira S.I., Olhero S.M., *ET AL.*: 'Synthesis, mechanical and biological characterization of ionic doped carbonated hydroxyapatite/β-tricalcium phosphate mixtures', *Acta Biomater.*, 2011, **7**, pp. 1835–1843

[21] Staní V., Dimitrijeví S., Stanković J., *ET AL.*: 'Synthesis, characterization and antimicrobial activity of copper and zinc-doped hydroxyapatite nanopowders', *Appl. Surface Sci.*, 2010, **256**, pp. 6083–6089

[22] White D.: 'Membrane bioenergetics: the proton potential', in: 'The physiology and biochemistry of prokaryotes' (Oxford University Press, New York, 2007), pp. 83–119

[23] Hu S., Chang J., Liu M., Ning C.: 'Study on antibacterial effect of 45S5 Bioglass', *Mater. Sci. Mater. Med.*, 2009, **20**, pp. 281–286

[24] Allan I., Newman H., Wilson M.: 'Antibacterial activity of particulate bioglass against supra- and subgingival bacteria', *Biomaterials*, 2001, **22**, pp. 1683–1687

[25] Green J.: 'Cytosolic pH regulation in osteoblasts', *Miner. Electrolyte. Metab.*, 1994, **20**, pp. 16–30

[26] Chakkalakal D.A., Mashoof A.A., Novak J., Strates B.S., McGuire M.H.: 'Mineralization and pH relationships in healing skeletal defects grafted with demineralized bone matrix', *J. Biomed. Mater. Res. Bull.*, 1994, **28**, pp. 1439–1443

[27] Okabe T., Sakamoto M., Takeuchi H., Matsushima K.: 'Effects of pH on mineralization ability of human dental pulp cells', *Basic Res. Technol.*, 2006, **32**, pp. 198–201

[28] Arnett T.R., Spowage M.: 'Modulation of the resorptive activity of rat osteoclasts small changes in extracellular pH near the physiological range', *Bone*, 1996, **18**, pp. 277–279

[29] Arnett T.R.: 'Acid–base regulation of bone metabolism', *Int. Congr. Ser.*, 2007, **1297**, pp. 255–267




doi: 10.1049/mnl.2013.0655